Physica B 526 (2017) 102–109

Contents lists available at ScienceDirect

Physica B

journal homepage: www.elsevier.com/locate/physb

Hyperfine field, electric field gradient, quadrupole coupling constant and magnetic properties of challenging actinide digallide

Sajid Khan[a,b,c,*], M. Yazdani-Kachoei[d,**], S. Jalali-Asadabadi[d], Iftikhar Ahmad[a,e]

[a] Center for Computational Materials Science, University of Malakand, Chakdara 18800, Pakistan
[b] Department of Physics, University of Malakand, Chakdara 18800, Pakistan
[c] Govt. Post Graduate College, Charsadda 24420, Pakistan
[d] Department of Physics, Faculty of Sciences, University of Isfahan, Hezar Gerib Avenue, Isfahan 81746-73441, Iran
[e] Abbottabad University of Science and Technology, Havelian, Abbotabad 22500, Pakistan

ARTICLE INFO

Keywords:
Structural properties
State-of-the-art calculations
Magnetic properties
Hyperfine field (HFF)
Electric field gradient (EFG)
Quadrupole coupling constant

ABSTRACT

In this paper, we explore the structural and magnetic properties as well as electric field gradient (EFG), hyperfine field (HFF) and quadrupole coupling constant in actinide digallide $AcGa_2$ (Ac = U, Np, Pu) using LDA, GGA, LDA+U, GGA+U and hybrid functional with Wu-Cohen Generalized Gradient approximation HF-WC. Relativistic effects of the electrons are considered by including spin-orbit coupling. The comparison of the calculated structural parameters and magnetic properties with the available experimental results confirms the consistency and hence effectiveness of our theoretical tools. The calculated magnetic moments demonstrate that UGa_2 and $NpGa_2$ are ferromagnetic while $PuGa_2$ is antiferromagnetic in nature. The EFG of $AcGa_2$ is reported for the first time. The HFF, EFG and quadrupole coupling constant in $AcGa_2$ (Ac = U, Np, Pu) are mainly originated from f-f and p-p contributions of Ac atom and p-p contribution of Ga atom.

1. Introduction

The quantum chemistry of actinide based molecules is challenging due to their complex electronic structures [1]. One of the interesting families of these challenging compounds is actinides digallide. The structural, electronic and magnetic properties as well as the hyperfine field (HFF) and electric field gradients (EFG) of the actinide based post transition metals have attracted considerable attention in modern condensed matter physics [2,3]. These materials have 5f electrons which exhibit some significant physical properties like Pauli paramagnetism, magnetic and electric hyperfine interactions, heavy fermions, spin fluctuation and unconventional superconductivity [4,5]. The 5f-electrons exhibit dual nature, some time behave like 4f- electrons [6–10], while in number of compounds it exhibit 3d- itinerant nature depending on their hosts [11–15].

Extensive experimental works have been reported about the importance of actinide based post transition metals $AcGa_2$ [Ac = U, Np, Pu] and other related compounds [16–18]. All the intermetallic compounds $AcGa_2$ crystallize in the hexagonal AB_2 type crystal structure with space group *P6/mmm*. It has been confirmed by single crystal X-ray diffraction experiments that the c/a ratio for these compounds increases when one moves from U to Pu, which implies that lattice parameter "c" increases more rapidly than lattice parameter "a" from U to Pu in the periodic table [2,3,19]. Honma et al. [2] and Yaar et al. [3] investigated the ferromagnetic nature of UGa_2 and $NpGa_2$ with Curie temperatures of 125 and 55 K, respectively, by Mössbauer as well as alternating and direct current techniques and found that the 5f-electrons of these compounds were localized. The X-ray diffraction study indicated that a slight orthorhombic distortion of UGa_2 occurred below 100 K [20]. The magnetic moment of the latter compound was obtained to be 2.7 μ_B/U by the magnetization study, which was close to 3.0 μ_B/U, as determined by the powder neutron diffraction study [21]. The experimentally investigated magnetic moment of $NpGa_2$ is 2.3 μ_B/Np [3]. Boulet et al. [19] studied the magnetic nature of $PuGa_2$ by means of susceptibility, magnetization and specific heat measurements and concluded that it had antiferromagnetic nature with Néel temperature of 74 K. The effective magnetic moment of Pu is measured experimentally by Boulet et al. to be 0.42 μ_B, which is much smaller than that of the Pu^{3+} free ion (2.6 μ_B) [19].

In this work, EFGs are investigated for these materials as a first time. The EFG is a physical quantity used to explore the geometry of the electron charge distribution around the nucleus of an atom or nuclei of a crystal [22]. The EFG has attracted enormous attentions for its interesting physics [23–27]. The quadrupole nuclei (with I ≥1) have

* Corresponding author at: Center for Computational Materials Science, University of Malakand, Chakdara 18800, Pakistan.
** Corresponding author.
E-mail addresses: skhan.ccms@gmail.com (S. Khan), yk.majid@gmail.com (M. Yazdani-Kachoei).

http://dx.doi.org/10.1016/j.physb.2017.09.052
Received 21 June 2017; Received in revised form 13 September 2017; Accepted 14 September 2017
Available online 18 September 2017

non-spherical structures due to their anisotropic nuclear charge distributions. These nuclei have nonzero electric quadrupole moments (Qs). The nuclear electric quadrupole interactions (QIs) have large applications and serve to investigate the distributions of electronic charges around the nuclear sites. It shows the bonding nature as well as shapes of orbitals in the compounds, their quadrupole frequency and quadrupole splitting. The QIs are also used for the characterization of surfaces, vacancies and impurities [28–32].

So far to the best of our knowledge no serious attention has been paid to the theoretical studies of intermetallic actinide digallide $AcGa_2$ system despite their fascinating properties such as heavy fermions, Pauli paramagnetism and spin fluctuation. In this study, we explore structural, magnetic, HFF and EFG of these materials in detail with the different flavors of exchange-correlations in density functional theory (DFT), *i.e.*, local density approximation (LDA), generalized gradient approximation (GGA), LDA plus Hubbard U correction (LDA+U), (GGA+U) and hybrid functional HF-WC. The relativistic effects can be significant in actinide post transition intermetallic compounds having 5f- electrons due to their large atomic numbers. Therefore, spin- orbit coupling (SOC) is included in our calculations to investigate the expected relativistic effects in these compounds.

2. Computational details

Our calculations have been performed in the framework of the DFT using the well-known all electron FP-LAPW+lo method implemented in WIEN2k package [33]. The unit cell is divided into two regions in LAPW+lo method, *i.e.*, non-overlapping muffin-tin spheres of radii R_{MT} around each atom and interstitial region. The wave functions inside the atomic spheres are expanded in spherical harmonics, while plane waves are used for the interstitial region [20,34]. In the present study, we deal with the actinide digallide which can behave as a strongly correlated system. The DFT is the base for majority calculations of the electronic structure of solids. The structural properties are investigated under the LDA and GGA [35,36]. These two approximations have well-known shortcomings for strongly correlated systems. Both approximations usually give good results for number of semiconductors and insulators, but they often fail to give satisfactory results for strongly correlated electron systems. The importance of the highly correlated systems and the shortcomings of these two approximations have encouraged researchers to think about solutions of these problems for such compounds [37]. The LDA results were tried to be improved by adding Hubbard potential [38,39], *i.e.*, the so-called LDA +U scheme. The LDA+U mostly yields good results for strongly correlated systems. The LDA+U total energy functional takes the form

$$E^{total}(\rho, \hat{n}) = E^{LDA}(\rho) + E^{ee}(\hat{n}) - E^{dc}(\hat{n}), \quad (1)$$

where $E^{LDA}(\rho)$ is the usual local density functional of the total electron spin density (ρ), E^{ee} is an electron-electron interaction energy and E^{dc} is the double counting correction term which accounts approximately for electron-electron interaction energy already incorporated in E^{LDA} [40]. In this study the value of U_{eff} = 0.20 Ry for UGa_2, 0.7 Ry for $NpGa_2$ and 0.20 Ry for $PuGa_2$ is considered for LDA+U approach. Our present calculations of $AcGa_2$ are also computed by using HF-WC. The EECE gives good result in case of $AcGa_2$ with α = 0.20 for UGa_2, 0.20 for $NpGa_2$ and 0.10 for $PuGa_2$. Moreira *et al.* proposed the hybrid functional with the following general form:

$$E_{xc}^{\text{onsite}-\text{HF}}[\rho] = E_{xc}^{\text{SL}}[\rho] + \alpha(E_x^{HF}[\Psi_{core}] - E_x^{SL}[\rho_{core}]), \quad (2)$$

where E_{xc}^{SL} is the semilocal (SL) functional and α is the fraction of Hartree-Fock exchange (between 0 and 1) [41–45]. It is identified that U, Np and Pu are strongly correlated systems with 5f electrons. Therefore, to take the better description of its properties into account LDA+U along with hybrid functional HF-WC calculations are necessary. In the present study, the maximum angular momentum quantum number for expanding the Kohn–Sham wave function within the muffin-tin sphere is confined to l_{max} = 10. The wave functions in the interstitial region are expanded in plane waves with a cutoff of $R_{MT}K_{max}$ = 9, where R_{MT} is the minimum muffin–tin radius in the unit cell. The charge density and potential are Fourier expanded in the interstitial region up to G_{max} = 12 (Bohr)$^{-1/2}$. The Brillouin zone integration is performed on a mesh of 15 × 15 ×13 k-points in the bulk of $AcGa_2$.

We carry out full relativistic calculations by including the spin-orbit coupling (SOC) in the Hamiltonian. Recent magneto crystalline anisotropy calculations [46] clearly show the importance of the relativistic effects for the electronic and magnetic properties investigations. In fact, the importance of relativistic effects strongly depends on the atomic number (Z), and increases by Z. This implies that the relativistic effects for Actinide-based compounds are crucial. However, the relativistic effects can be safely neglected when the speed of electron is much less than the speed of light speed in vacuum (c). Therefore, in the WIEN2k code the relativistic corrections are only considered for the electrons in the muffin-tin spheres and these effects are safely neglected for the electrons in the interstitial region. This is so, because in the interstitial region the electrons are far from the core region and thereby their speed are much smaller than c, while this may not be the case for the electrons in the muffin-tin spheres. In the WIEN2k code the method of including relativistic effects in the core electrons differs from that of the valence electrons. The core states are considered fully relativistically, while for the valence states the relativistic effects are approximated using the second variational method including the SOC [47,48]. When including the SOC within the second variation step, the size of the new basis set is determined by the E_{max} parameter [46]. The E_{max} determines the maximum energy for which all the scalar-relativistic eigen states are included. To increase our accuracy, we set the E_{max} to 10 Ry, while its default is 1.5 Ry. The speed of our SOC calculations could be speed up by reducing the E_{max} parameter, if it was permitted to add the relativistic local orbitals (RLO's). However, since the EFG and the dipolar HFF are the main goals of this study, we avoid considering the RLO's as additional basis functions [49] for our SOC calculations due to the known limitations of the WIEN2k code. The direction of magnetization is also selected to be along the [001].

3. Structural properties

$AcGa_2$[Ac = U, Np, Pu]intermetallic compounds exhibit AB_2 type hexagonal crystal structures with space groupP6/mmm-D (191), with atomic positions Ac in 1(a); [0, 0, 0] and Ga in 2(d) [1/3, 2/3, 1/2]; [2/3, 1/3, 1/2] [50]. The experimental lattice constants of UGa_2 compound are a = b = 4.21 Å, c = 4.01 Å and its c/a ratio is 0.953. The experimental lattice constants and c/a are a = b = 4.259 Å, c = 4.077 Å, c/a = 0.957 for $NpGa_2$ and a = b = 4.254 Å, c = 4.124 Å, c/a = 0.969 for $PuGa_2$ [2,3,19,20]. We have started from experimental lattice parameters and relaxed the unit cell by minimizing the total energy *versus* unit cell volume and fitted the results with a Birch-Murnaghan equation of state. From the ground state volumes, the structural parameters, including lattice constants, bulk moduli and their derivatives are obtained [51]. For optimization of $AcGa_2$unit cell we used 2-D optimization package using different potential which are shown in Table 1. Both LDA and GGA underestimate the lattice constants 7–30% especially for c and 0.5–1.4% for a and b as shown in Fig. 1(a). To improve the results, we used other functional like LDA+U and GGA+U which are more appropriate for the heavy fermions. The c/a ratio has been calculated computationally. The results of LDA and GGA are far away from the experimental curve while the LDA+U results are well consistent to the experimental data which exhibits that LDA+U can well predict the structural properties of f-electrons family. As shown in Table 1, the 2D calculations can give satisfactory results which are very close to the experimental data and thereby well optimize the system. It is concluded that calculated lattice constants of $AcGa_2$ by LDA+U are suitable. The bulk modulus which shows the strength and hardness of a

Table 1
Calculated lattice constants (Å), bulk moduli (GPa), derivative of bulk moduli as well as c/a ratio of $AcGa_2$ by different potentials and comparison with experimental results.

Flavors	Lattice parameter	UGa_2	± % error	$NpGa_2$	± % error	$PuGa_2$	± % error
GGA	a = b (Å)	4.1751	0.8	4.2448	1.40	4.2760	0.5
	c (Å)	3.8567	15	3.7678	30.0	3.7971	7.0
	c/a	0.9238	2.0	0.8871	7.00	0.8880	8.0
	B (GPa)	80.978		85.042		88.282	
	B/	1.9111		3.7585		5.4999	
LDA							
	a = b (Å)	4.1217	8.0	4.1896	6.00	4.2304	0.5
	c (Å)	3.8600	15	3.7468	8.00	3.7609	8.0
	c/a	0.9365	1.5			0.8890	8.0
	B (Gpa)	104.25		112.05		111.71	
	B/	4.2583		8.8189		7.4361	
LDA+U	a = b	4.2290	0.4	4.2590	0.00	4.2600	0.1
	c (Å)	4.0090	0.1	4.0760	0.02	4.1300	0.1
	c/a	0.9470	0.5	0.9570	0.00	0.9690	0.0
	B (Gpa)	137.57		114.58		112.31	
	B/	3.0288		5.2370		5.4530	
GGA+U	a = b	4.2330	0.5	4.2480	0.02	4.3120	4.0
	c (Å)	4.0160	0.6	4.0570	0.40	4.1030	0.1
	c/a	0.9480	0.4	0.9550	0.20	0.9520	1.0
	B (Gpa)	87.158		113.29		119.07	
	B/	3.9321		4.3420		4.7650	
Exp a = b Åc Å		$4.21^{(2)}4.01^{(2)}$		$4.26^{(3)}4.08^{(3)}$		$4.25^{(19)}4.12^{(19)}$	
Exp c/a		0.9520		0.9570		0.9690	

material are investigated for $AcGa_2$. The bulk moduli are calculated by different exchange-correlation functional as shown in the Table 1. The calculated bulk moduli are inversely related to the lattice constants. This shows that the compressibility is proportional to the lattice constants. The LDA+U confirm this relation as shown in Fig. 1(b). The results of the other functional do not show this behavior. The calculated result of LDA+U shows that hardness decreases while the compressibility increases from uranium to plutonium.

4. Magnetic properties

The magnetic behavior is an interesting property of $AcGa_2$ [Ac = U, Np, Pu], and therefore its detail study has significant importance. To investigate the magnetic phase of $AcGa_2$, we optimized double cell of these compounds by LDA+U. Hence, we found the minimum energies of UGa_2 and $NpGa_2$ to be − 127805.97598684 and − 130990.79156800 Ry in the ferromagnetic phase, respectively, see Table 2. The minimum energy of $PuGa_2$ is calculated to be − 134239.55635983 Ry in antiferromagnetic phase, as shown in Table 2. To investigate the interstitial and individual atomic spin magnetic moments per unit cell of $AcGa_2$, we utilize different functionals like, LDA+U and hybrid functional HF-WC. To consider orbital magnetic moments of $AcGa_2$, we also include spin-orbit coupling (SOC) by performing LDA+U+SOC and HF+SOC. Our calculated values of magnetic moments for $AcGa_2$ by LDA are not consistent to experimental results. This is due to the well-known problem of LDA which indicates that this local approximation is not fully appropriate for strongly correlated d and f electrons. The main deficiency is the self-interaction error (SIE) contained in LDA and GGA functional.

The results are also checked by adding U to these approximations or using hybrid functional [52]. The LDA+U and HF-WC results are also

Table 2
Ground state energy of 2 × 1 × 1 super cell of $AcGa_2$ (Ac = U, Np, Pu).

Compounds	E_{AFM} (Ry)	E_{FM} (Ry)	$E_{NON-MAG}$ (Ry)
UGa_2	− 127805.8907245	− 127805.9759868	− 127805.8806342
$NpGa_2$	− 130990.4886088	− 130990.7915680	− 130990.4235672
$PuGa_2$	− 134239.5563598	− 134239.1301245	− 134239.3124523

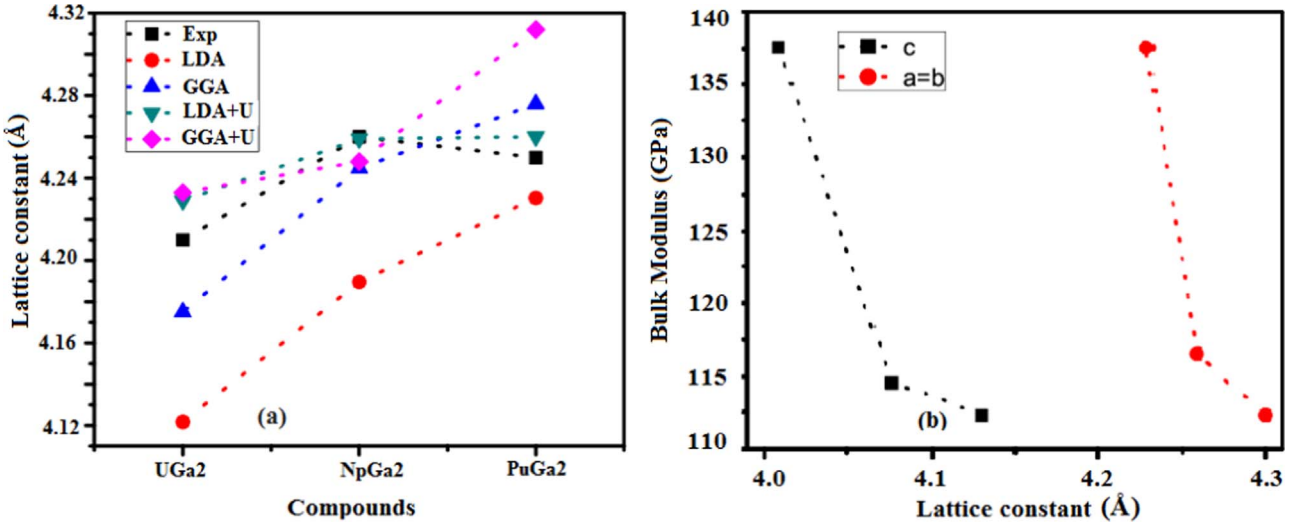

Fig. 1. (a) Comparison of calculated and experimental lattice constant of $AcGa_2$ compounds (b). The bulk modulus against lattice constant (a = b and c).

Table 3
Calculated spin magnetic moments inside all of the muffin-tin spheres, interstitial and orbital magnetic moment of $AcGa_2$ (Ac = U, Np, Pu) compounds in unit cell by LDA+U, HF-WC LDA+U (SOC) and HF-WC (SOC) in the unit of bohar magneton in (001) plane.

Compounds	Sites	Magnetic moment							
		LDA+U	HF- WC	LDA+U (SOC)			HF- WC + (SOC)		
		Spin (μ_B)	Spin (μ_B)	Spin (μ_B)	μ_{Orb}	$\lvert\mu_{tot}\rvert$	Spin (μ_B)	μ_{Orb}	$\lvert\mu_{tot}\rvert$
UGa_2	M^{int}	0.269	0.435	0.274	–	0.274	0.244	–	0.244
	M^{U}	2.117	2.045	2.024	− 4.374	− 2.35	1.641	− 4.296	2.65
	M^{Ga}	− 0.013	0.031	− 0.013	− 0.009	− 0.02	− 0.009	− 0.007	0.02
	M^{tot}	2.373	2.511			− 2.09			2.42
Exp	3.0/U [20]								
	2.7/U [21]								
	M^{int}	0.915	0.231	0.350	–	0.350	0.2167	–	0.217
$NpGa_2$	M^{Np}	4.115	3.831	3.019	− 5.624	− 2.61	3.029	− 5.316	2.29
	M^{Ga}	0.019	0.032	− 0.007	− 0.004	− 0.01	− 0.017	− 0.008	0.03
	M^{tot}	5.049	4.094			− 2.27			2.09
Exp	2.39/Np[3]								
	2.6/$NpGa_2$[3]								
$PuGa_2$	M^{int}	0.686	0.325	0.447	–	0.447	0.213	–	0.213
	M^{Pu}	5.057	4.923	4.728	− 4.342	0.386	4.449	− 4.279	0.17
	M^{Ga}	− 0.047	− 0.021	− 0.017	− 0.007	− 0.03	− 0.023	− 0.006	0.02
	M^{tot}	5.696	5.227			0.839			0.35
Exp	0.42 [19]								

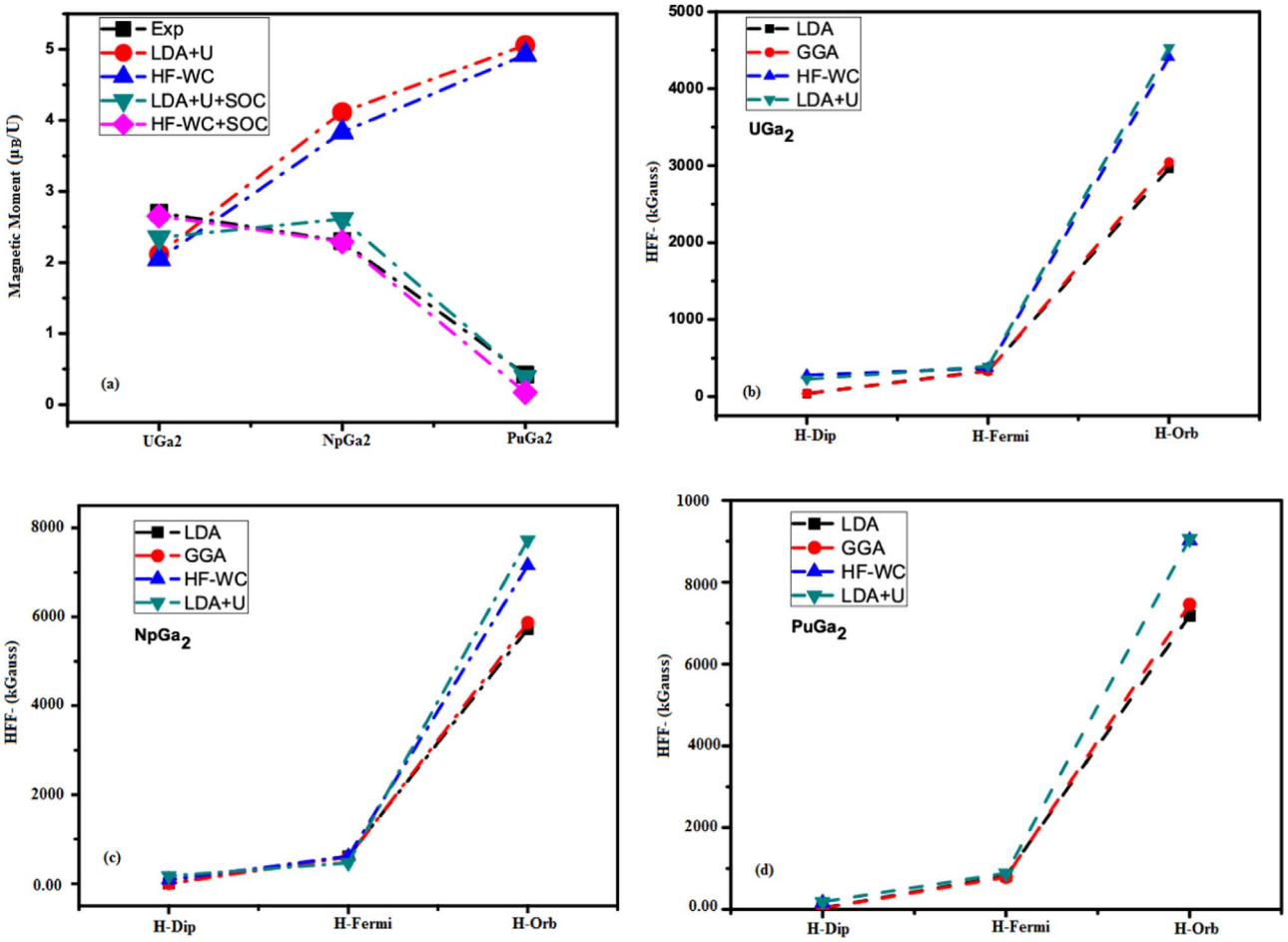

Fig. 2. (a) Comparison of experimental and calculated magnetic moment of uranium atom in $AcGa_2$. Fig. 2(b, c, d) exhibit the dipolar, orbital and Fermi contact HFF at actinide and gallium site.

shown in the Table 3, which are not significant but the results of SOC in these materials are very appreciable. This means that SOC treats well with the number of fermions in d and f orbitals. Our calculated magnetic moments for UGa_2, $NpGa_2$ and $PuGa_2$ by different potentials are shown in Table 3 as well as in Fig. 2(a). To calculate the orbital magnetic moment the SOC calculation is also performed for UGa_2. The LDA+U+SOC scheme gives the spin, orbital and total magnetic moments of Uranium atom to be 2.024, − 4.374 and 2.35 μ_B/U, respectively in agreement with Lawson et al. [21] and Andreev et al. results [20]. The foremost contribution in spin magnetic moments

originates from the non-spherical orbital electrons $5f^{+3}$ [U^{+3}]. The Ga magnetic moment is negligible due to nearly closed 3d and 4p shells [53]. It is seen that SOC has considerable effects on the results of heavy fermion compounds. The calculated magnetic moments of ferromagnetic $NpGa_2$ and antiferromagnetic $PuGa_2$ have been calculated by different flavors with addition of SOC. The LDA+U and HF-WC result for $NpGa_2$ agrees with the experimental value. The local magnetic moment by neptunium atom is due to Np^{+3} valence electrons while the s, p and d orbital magnetic moments almost cancel the effects of each other. The ground state term value of Np^{+3} which is highly correlated $5f^4$ is $^5I_4$ with $L = 6$, $S = 2$ and $J = 4$. The Landé g factor is $g_L=\frac{3}{5}$ and the effective magnetic moment is $m_o = gJ\mu_B = 2.4\ \mu_B$. The electronic and magnetic properties of $NpGa_2$ are due to the 5f localized and three conduction electrons of Np^{+3}ions. $PuGa_2$ is antiferromagnetic with experimental magnetic moment of 0.42 μ_B. The HF-WC+SOC calculated orbital and spin magnetic moments are shown in Table 3. The calculated small effective magnetic moment of $PuGa_2$ is 0.386 μ_B which is very far away from theoretical magnetic moment 2.6 μ_B for Pu^{+3} while it is close to the experimental result. This can be taken as an indication to the fact that the 5f electrons in $PuGa_2$ are delocalized or band like. To investigate the antiferromagnetic nature of $PuGa_2$, double cell calculation has been performed as shown in Table 4. The up and down magnetic moments of Pu completely cancel each other and as a result the net magnetic moment in double cell is zero. One of the basic questions arising in the field of actinide intermetallic systems is whether the 5f electrons are localized or itinerant in nature. To clarify this, as shown in Table 3, the significant magnetic moments of UGa_2 and $NpGa_2$ by LDA+U+SO and HF-WC+SO suggest that the 5f electrons are mostly localized at the uranium and neptunium atomic sites, while the less effective moment of $PuGa_2$ extracted from different potentials propose the delocalization of 5f electron.

5. Hyperfine field

Magnetic hyperfine fields arise due to the interaction of nuclear magnetic dipole moment μ_N and additional nuclear magnetic field created by the electron clouds around the nucleus in the crystal. The total Hyperfine field (HFF) as well as the electric-field gradient (EFG) interaction provide information about nucleus and its surrounding electrons charge distribution. They can be measured by various experimental techniques like Mössbauer spectroscopy, perturbed angular correlation or nuclear magnetic resonance. The HFF consists of orbital, dipolar and Fermi contact field. The Fermi contact (FC) which is the sum of core and valence HFF. Fermi contact portion of hyperfine field (HFF_{FC}) can be calculated by the upward and downward spin density of electrons [$n_s^{\uparrow\downarrow}$] at the nuclear site using Pauli approximation within the non-relativistic limit

$$HFF_{FC} = \frac{8\pi}{3}\mu_B^2[\rho_s^{\uparrow}(0)-\rho_s^{\downarrow}(0)]. \quad (3)$$

The relativistic correction has been obtained by taking average over spin density and Thomson radius $r_T = Ze^2/mc^2$. In this work, special concentration are devoted to the question that cannot be directly answered by the experiments. The question is that which contributions, *i.e.*, Fermi, dipolar or orbital, are dominantin the magnetic HFF and what the source of a nonzero HFF is at the Ac and Ga sites. To calculate

Table 4
Net magnetic moment of double cell of $PuGa_2$.

Sites	LDA	HF-WC
M^{Int}	0.00000	0.00000
Pu^{up}	− 0.00572	0.00178
Pu^{dn}	0.00572	− 0.00178
Ga	0.00000	0.00000
M^{total}	0.00000	0.00000

Table 5
Calculated Fermi, Orbital and Dipolar contributions to the total hyperfine field (HFF) in KGAUSS at the Ac (U, Np, Pu) and Ga atoms in $AcGa_2$ compounds by different exchange potentials LDA, GGA, HF- WC and LDA+U in the presence of spin-orbit coupling.

Compounds	HFF (KGAUSS)	LDA	GGA	HF-WC	LDA+U
UGa_2 -	$\lvert H_{hf}^{Tot}\rvert$	− 3333.66	− 3414.58	− 5053.86	− 5149.72
UGa_2 -U	H_{hf}^{Fer}	− 335.592	− 327.472	− 368.891	− 391.847
UGa_2 -U	H_{hf}^{Orb}	− 2959.93	− 3045.82	− 4407.24	− 4533.15
UGa_2 -U	H_{hf}^{Dip}	− 38.1293	− 41.2880	− 277.731	− 224.721
UGa_2 -Ga	$\lvert H_{hf}^{Tot}\rvert$	− 63.2850	− 72.9223	− 106.664	− 105.205
UGa_2 -Ga	H_{hf}^{Fer}	− 60.1000	− 70.1501	− 95.6932	− 91.2581
UGa_2 -Ga	H_{hf}^{Orb}	− 2.76600	− 2.33982	− 8.23800	− 9.82100
UGa_2 -Ga	H_{hf}^{Dip}	− 0.41900	− 0.43251	− 2.73300	− 4.12600
$NpGa_2$ -	$\lvert H_{hf}^{Tot}\rvert$	− 6341.49	− 6465.98	− 7851.08	− 8362.76
$NpGa_2$ -Np	H_{hf}^{Fer}	− 612.993	− 591.042	− 613.527	− 466.185
$NpGa_2$ -Np	H_{hf}^{Orb}	− 5725.07	− 5874.32	− 7153.43	− 7724.96
$NpGa_2$ -Np	H_{hf}^{Dip}	− 3.42210	− 0.61610	− 84.1213	− 171.620
$NpGa_2$ -Ga	$\lvert H_{hf}^{Tot}\rvert$	− 110.825	− 127.136	− 122.570	− 32.4152
$NpGa_2$ -Ga	H_{hf}^{Fer}	− 103.464	− 120.836	− 108.841	− 24.6652
$NpGa_2$ -Ga	H_{hf}^{Orb}	− 5.74013	− 5.27421	− 10.3732	− 4.17100
$NpGa_2$ -Ga	H_{hf}^{Dip}	− 1.62081	− 1.02621	− 3.35621	− 3.58200
$PuGa_2$ -	$\lvert H_{hf}^{Tot}\rvert$	− 7970.45	− 8222.93	− 9760.51	− 9764.38
$PuGa_2$ -Pu	H_{hf}^{Fer}	− 825.341	− 791.074	− 898.926	− 888.007
$PuGa_2$ -Pu	H_{hf}^{Orb}	− 7181.42	− 7460.99	− 9021.48	− 9065.03
$PuGa_2$ -Pu	H_{hf}^{Dip}	36.3152	29.1321	159.890	188.660
$PuGa_2$ -Ga	$\lvert H_{hf}^{Tot}\rvert$	− 129.246	− 154.207	− 145.441	− 147.032
$PuGa_2$ -Ga	H_{hf}^{Fer}	− 125.909	− 144.699	− 136.232	− 140.701
$PuGa_2$ -Ga	H_{hf}^{Orb}	− 5.68620	− 5.67431	− 8.29321	− 9.36321
$PuGa_2$ -Ga	H_{hf}^{Dip}	2.34913	− 3.83421	− 0.91643	3.03214

HFF we used the FP-LAPW method as implemented in WIEN2k. The total hyperfine field (HFF) is calculated by the following formula [54–57] including core (H_{hf}^{c}), valence (H_{hf}^{v}), orbital (H_{hf}^{orb}) and dipolar (H_{hf}^{dip}) contributions:

$$H_{hf}^{tot} = H_{hf}^{c}+H_{hf}^{v}+H_{hf}^{orb}+H_{hf}^{dip}. \quad (4)$$

Our calculated total HFF and its partial components are tabulated in form of Table 5. For each atom of the $AcGa_2$ compound within LDA, GGA, HF-WC and LDA+U. Due to the opposite signs of the valence and core electrons the Fermi contact fields at U, Np and Pu sites are small in magnitude. The inner s- and polarized f-shell electrons interact to each other and contribute in core HFF, while the valence HFF originates due to the hybridization of local polarized f, valence s and polarized valence shell electrons of neighboring atoms. Hence, it is concluded that Fermi contact HFF is determined from the contribution of local and neighboring atomic magnetic moments. The valence contribution in HFF is smaller in contact field than core contribution in Ac (Ac = U, Np, Pu) and majority of inner magnetic dipole moments of electrons align in one direction while they are smaller in opposite direction. The orbital HFF is very large in magnitude as shown in the Table 5 and Fig. 2. (b–d). The dominant contribution is due to the f- and p- electrons. There is an increasing trend in orbital magnetic moment at actinide site, due to the varying of electrons in f-states. It is suggested that the origin of the orbital and dipolar contribution of the HFF is exchange interaction of p-and f-shells in uranium, neptunium and plutonium site, while p- and d- orbital contributed in gallium. The total HFF also increase from uranium to plutonium an $AcGa_2$ series as shown in Table [5].

The dipolar magnetic moment which is due to spin of electron has been calculated as shown in Table 5 and Fig. 2(b–d). As the s- and p-orbitals of actinide atom are filled, the dipolar HFF for these are negligible while the major donation arises due to d- and f-orbitals,

Table 6
Calculated EFGs at Ac (U, Np, Pu) and Ga sites by different exchange-correlation functionals in the unit of 10^{21} V/m^2 with Quadrupole coupling constants in MHz.

Compounds	Different functional	V_{zz}^{tot}	V_{zz}^{p-p}	V_{zz}^{s-d}	V_{zz}^{d-d}	V_{zz}^{p-f}	V_{zz}^{f-f}	V_{zz}^{val}	V_{zz}^{lat}	C_q MHz
UGa2-U	LDA	− 0.0942	3.5136	− 0.1781	− 1.7707	0.0085	− 1.6730	− 0.0997	0.0055	
UGa2-Ga	LDA	− 1.6355	− 0.7951	0.0277	− 0.7258	0.0460	0.0009	− 1.4463	− 0.1892	
UGa2-U	GGA	0.6131	2.4683	− 0.1467	− 1.6506	0.0023	− 0.0781	0.5952	0.0179	
UGa2-Ga	GGA	− 1.4969	− 0.6191	0.2973	− 0.7606	0.0257	0.0009	− 1.0557	− 0.4411	
UGa2-U	LDA+SOC	1.0882	− 0.2607	− 0.0685	− 1.8948	− 0.0141	3.2949	1.0568	− 0.0314	128
UGa2-Ga	LDA+SOC	− 1.1692	− 0.3194	0.0277	− 0.7350	0.0458	0.0007	− 0.9802	− 0.1890	4.00
UGa2-U	GGA+SOC	1.3950	0.1902	− 0.0621	− 1.8080	− 0.0119	3.4408	1.7490	− 0.3540	166
UGa2-Ga	GGA+SOC	− 0.9543	− 0.0695	0.0298	− 0.7577	0.0456	0.0009	− 0.7509	− 0.2034	2.00
NpGa2-Np	LDA	1.4170	4.2353	0.0703	− 1.3045	0.1190	− 1.4550	1.6651	− 0.2481	
NpGa2-Ga	LDA	− 0.5479	0.1429	0.1396	− 0.7915	0.0451	0.0009	− 0.4630	− 0.0849	
NpGa2-Np	GGA	1.8549	3.1603	− 0.0370	− 1.2609	0.0039	− 0.0161	1.8500	0.0048	
NpGa2-Ga	GGA	− 0.2328	0.4862	0.0283	− 0.7168	0.0449	0.0009	− 0.1564	− 0.0764	
NpGa2-Np	LDA+SOC	3.3704	10.468	− 0.1627	− 0.6972	0.0173	− 6.2754	3.3500	0.0204	314
NpGa2-Ga	LDA+SOC	− 0.3561	0.0597	0.0269	− 0.6387	0.0453	0.0008	− 0.5060	0.1499	0.80
NpGa2-Np	GGA+SOC	3.3704	10.499	− 0.1565	− 0.6491	0.0173	− 6.2870	3.4237	− 0.0533	314
NpGa2-Ga	GGA+SOC	− 0.4562	0.2755	0.0287	− 0.6267	0.0456	0.0008	− 0.2760	0.1802	1.00
PuGa2-Pu	LDA	1.9480	4.1413	0.0344	− 1.3456	− 0.0002	− 0.8886	1.9413	0.0067	
PuGa2-Ga	LDA	1.1224	1.7658	0.0258	− 0.5472	0.0453	0.0008	1.2905	− 0.1681	
PuGa2-Pu	GGA	1.6831	5.4510	0.0006	− 1.9716	0.0049	− 2.4374	1.0475	0.6356	
PuGa2-Ga	GGA	1.4232	2.0832	0.4634	− 0.5634	0.0452	0.0009	2.0293	− 0.6061	
PuGa2-Pu	LDA+SOC	4.1022	20.009	− 0.2344	− 0.6621	0.0390	− 14.833	4.3185	− 0.2163	229
PuGa2-Ga	LDA+SOC	0.8838	1.5806	0.0154	− 0.5984	0.0451	0.0008	1.0435	− 0.1597	4
PuGa2-Pu	GGA+SOC	4.1513	20.156	− 0.2376	− 0.5512	0.0360	− 15.039	4.3638	− 0.2125	232
PuGa2-Ga	GGA+SOC	0.6213	1.2990	0.0264	− 0.5812	0.0451	0.0008	0.7901	− 0.1688	2.00

while p-orbital contribution is dominant in gallium.

We see that by HF-WC and LDA+U the HFF steadily rises when one goes from UGa_2 to $PuGa_2$. The systematic enhancement in the HFF at the Ac site with increased atomic number is due to the increased spin magnetic moment on the Ac site. The comparison of the results shows the large increase of the HFF on the Ac site from UGa_2 to $PuGa_2$ as shown in Table 5. The large value of Pu is due to the delocalized of 5f electrons. The valence electrons in U and Np atoms are localized in contrast to Pu atom. At the Ac site of the $AcGa_2$ compounds, the HFF is larger for Ac = Pu than those for Ac = U and Np due to the larger number of f-electrons in Pu atom than those in U and Np atoms.

If the local moment of the specific atom increases, the core polarization will be large in magnitude due to the exchange interaction of the polarized electrons with the neighboring s and p orbitals of the core. Hence, the systematic increase observed of the core contribution to the HFF at the Ac site as one goes from UGa_2 to $PuGa_2$ can be understood in terms of the increasing trend in local moment on the Ac site.

Since the local moments on the Ga site are negligible, the core and dipolar contributions to the HFF at this site are small in magnitude. The HFF at Ga site in $PuGa_2$ is more in magnitude than the others due to the overlapping of delocalized 5f valence electrons of Pu. The large value of Fermi contact at the Ac site can be qualitatively explained as follows. The majority spin s electrons in the core will be pulled into the region of the spin-polarized d- and f-shells, since the exchange interaction is attractive, whereas the minority electrons will be repelled from the d- and f- shells [56]. The HFF and atomic magnetic moments ratio [C=HFF/μ_B] is increased from U to Pu. The C values vary due to variation of 5 f electrons in valence orbital. The positive C shows that core polarization is parallel to the local moments [55]. These are the suggested HFF values in $AcGa_2$ family for nuclear experimentalists to measure magnetic hyperfine interaction energy at actinide and gallium sites.

6. Electric field gradient (EFG)

EFG is a local property of materials and defined as the second partial derivative of the potential V evaluated at position of the nucleus. It is a traceless symmetric tensor of rank two. The main component of total EFG (V_{zz}^{total}) can be calculated by the sum of its valence and lattice contributions:

$$V_{zz}^{total} = V_{zz}^{val} + V_{zz}^{latt}, \tag{5}$$

where valence EFG (V_{zz}^{val}) originates from anisotropic electron (non-spherical) charge distribution inside the atomic spheres while V_{zz}^{latt} is due to the interstitial region. The principle component of the EFG (V_{zz}) can be obtained from the L = 2 and M = 4 component of the potential expansion inside the muffin-tin spheres as follows: [28,57–59]

$$V_{zz} = \lim_{r\to 0}\left[\frac{5}{4\pi}\right]^{1/2}\left[\frac{V_{20}(r)}{r^2}\right]. \tag{6}$$

Eq. (6) shows that major axis of EFG tensor points in the z-direction, where V_{20} is the radial potential and can be calculated as

$$V_{20}(r=0) = \frac{4\pi}{5}\int_0^{R_{MT}}\frac{\rho_{20}}{r}dr - \frac{4\pi}{5}\int_0^{R_{MT}}\frac{\rho_{20}}{r}\left(\frac{r}{R_{MT}}\right)^5 dr + 4\pi\sum_k V(k)J_2(kR_{MT})Y_{20}(\hat{k}), \tag{7}$$

where the first term in Eq. (7) is contributed in EFG due to valence or quasi-core in muffin-tin sphere. The second and third terms summation shows the lattice contribution in EFG due to the interstitial region, where ρ_{20} is the L = 2 and M = 0 of density expansion while $J_2(kR_{MT})$ is the spherical Bessel function and R_{MT} is the Muffin-tin (MT) sphere radius. The value of EFG of a single atom is different in different materials. It means that the EFG for a specific atom can be small or zero in one compound, while it can be non-zero and large in another compound, therefore EFG can be considered as the fingerprint for each substance [60]. Theoretically, knowledge of the EFG's at the atomic sites suffices to predict the U, Np and Pu nuclear quadrupole coupling constant (NQCC) as well as Mössbauer quadrupole splitting Δ in the compound [61]. The quadrupole splitting is given by

$$\Delta = \left|\frac{e^2qQ}{2}\right|\sqrt{1+\frac{\eta^2}{3}}, \tag{8}$$

where eq is the largest eigenvector of the EFG tensor, η is asymmetry parameter and Q is nuclear quadrupole moment [62]. Electric field gradient of actinide digallide ($AcGa_2$) is examined for the first time by using different potential like LDA, GGA, LDA+SOC and GGA+SOC. Owing to some limitations of LDA and GGA as discussed previously we

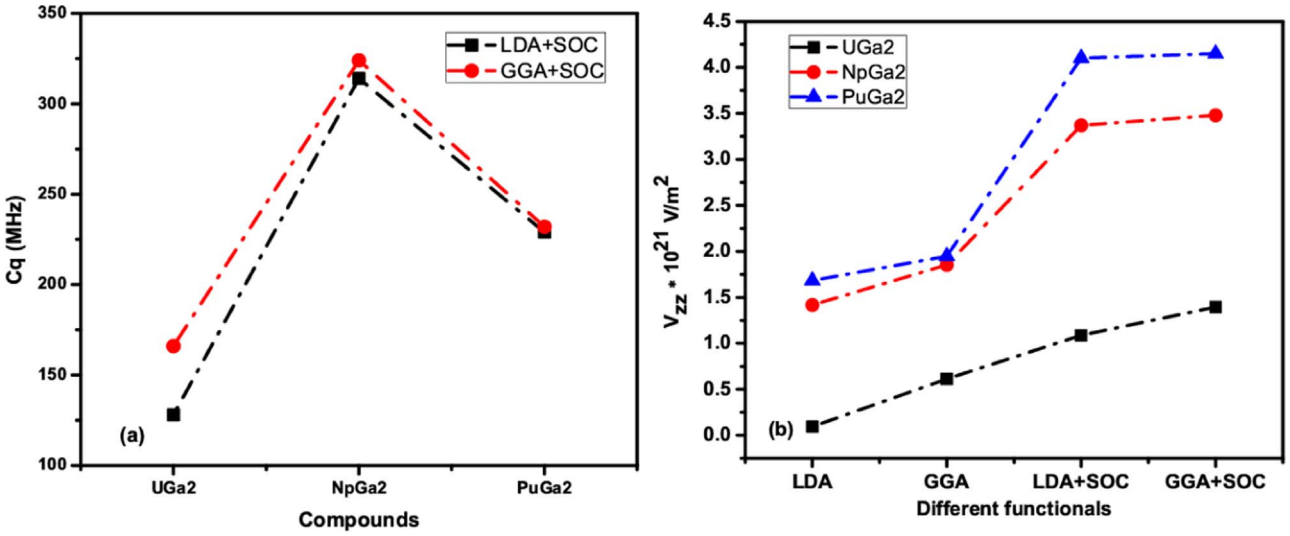

Fig. 3. (a) Variation of quadrupole coupling constant against different actinide site. (b) Principal component of EFG at uranium, neptunium and plutonium site with different functionals.

mention here only the results of LDA+SOC and GGA+SOC. The calculated total, lattice and valence contributions as well as different characters of EFG at both Ac and Ga sites in $AcGa_2$ within various functional are tabulated in Table 6. According to our calculated data the total EFG (V_{zz}^{tot}) at Ac site is increased from U to Pu within all considered approaches. The positive EFG values of actinides exhibit prolate distribution of electron while Ga has oblate distribution except for $PuGa_2$. It is noticed that the s-d and p-f contributions of Ac in $AcGa_2$ (Ac = U, Np, Pu) are small compared to the p-p, d-d and f-f contributions. This exhibits that the leading contribution to EFG comes from electrons with strong p-p, d-d and f-f characters. The EFG due to different energy states at Ga site is also shown in Table 6, where the dominant contribution in the electric field gradient is due to p-p (4p) and d-d (3d) characters which confirm the aspherical electronic distribution. In $AcGa_2$ Ga atom has 3d complete shell, and thereby the d orbital is nearly spherically symmetric. The small d- contribution is the consequences from an extension of the tails of the wave functions arriving from other atomic spheres into the Ga atomic sphere. The majority EFG of U in UGa_2 originates from the valence characters of p-p and f-f orbitals which specify the non-spherical distribution of charge. In case of $NpGa_2$ the contributions of d-d EFG at Np site are small compared to 5f and 6p, while f-p and s-d contributions are negligible in magnitude. The total EFG of Np is positive which predicts the prolate shape. The valence and lattice EFGs of Pu atom in $PuGa_2$ are 4.3185×10^{21} V/m^2, 4.363×10^{21} V/m^2 and -0.2163×10^{21} V/m^2 and -0.2125×10^{21} V/m^2 by LDA+SOC and GGA+SOC. All the p-, d-, and f-orbitals of Pu are non-spherical in nature, as tabulated in Table 6. However, the large EFG at Ga site in $PuGa_2$, 0.8838 and 0.6213×10^{21} V/m^2, mainly originates from the non-spherical p-orbital so that contributions of the d- and f-orbitals can be almost neglected.

The EFG increases when we use LDA+SOC and GGA+SOC instead of LDA and GGA, as shown in Fig. 3(b), which is consistent to other results. The nuclear quadruple coupling constant (C_q) is a significant parameter used for the purpose to calculate Mössbauer quadrupole splitting in atom or compound. The nuclear electric quadrupole moment (Q) of U, Np, Pu and Ga are 4.936, 3.866, − 2.3191 and 0.105 barn, respectively [63,64]. The nuclear electric quadrupole coupling constants ($C_q = eV_{zz}Q/h$) of $AcGa_2$ (Ac = U, Pu, Np) have been calculated for the first time for Ac and Ga atoms which have significant role in NMR and NQR literature. The major part of the quadrupole interaction energy is contributed by aspherical 5f and 6p states of electrons which diffuse around the nuclei of Ac in $AcGa_2$. The quadrupole coupling constant of U and Ga in UGa_2 are 128 MHz and 4.00 MHz and 166 MHz and 2 MHz by LDA+SOC and GGA+SOC. The major contribution in NQCC is due to the valence non-spherical V_{zz}^{d-d} and V_{zz}^{f-f} EFGs. The quadrupole interaction energies at U, Np and Pu are due to the result of electric quadrupole moment of nuclei and its corresponding valence EFGs of 6p and 5f electrons, while in case of Ga the interaction is due to the 3d and 4pelectrons. The EFG and Q interact to each other due to the quadrupole interaction energy. By the relation, one can easily calculate the quadrupole interaction energy at every site. The quadrupole coupling constant C_q and EFGs increased from uranium to plutonium in $AcGa_2$ series as shown in Figs. 3(a) and (b). The quadrupole interaction energy at different actinide site can easily obtain from $E = hC_q$.

7. Conclusion

We used the density functional calculations to study structural, magnetic, hyperfine and electric field gradient (EFG) properties of the bulk hexagonal $AcGa_2$ [Ac = U, Np,Pu]. In the bulk calculations, we applied LDA, LDA+U, GGA, GGA+U and HF-WC Hybrid functionals. We observe that GGA+U and LDA+U can reproduce the experimental lattice parameters, while LDA+U+SO and HF-WC+SO give appropriate magnetic moments. The considerable total magnetic moments of UGa_2 and $NpGa_2$ by LDA+U+SO and HF-WC+SO propose that the 5f electrons are mostly localized at the uranium and neptunium atomic sites, while the less effective moment of $PuGa_2$ extracted from different functionals proposes delocalization of its 5f-electrons. The EFGs are calculated for the first time for these compounds. The EFGs of the individual orbitals as well as nuclear quadrupole coupling constants of Ac and Ga are investigated for the first time which shows the anisotropy of charges and interaction energy. Our analysis reveals that the value of total EFG at Ac site as well as quadrupole coupling constants increase with increase of atomic number from U to Np, and then decrease upto Pu. Our results also show the prolate distribution of electron at Ac site for all the considered compounds. The EFGs at Ga site is negative for the ferromagnetic UGa_2 and $NpGa_2$ compounds, while it is positive for the antiferromagnetic $PuGa_2$ case. The EFGs at Ga site have mainly d-d character for both high and low localized regimes.

References

[1] M. Pepper, B.E. Bursten, Chem. Rev. 91 (1991) 719–741.
[2] T. Honma, Y. Inada, R. Settai, S. Araki, Y. Takiwa, T. Tateuchi, H. Sugawara, H. Sato, K. Kuwahara, M. Yokoyama, H. Amitsuka, T. Sakakibara, E. Yamamoto,

Y. Haga, A. Nakamura, H. Harima, H. Yamagami, J. Phys. Soc. Jpn. 26 (2000) 69.
[3] I. Yaar, S. Fredo, J. Gal, W. Potzel, G.M. Kalvius, F.J. Litterst, Phys. Rev. B 45 (1992) 9765.
[4] D. Koelling, B.D. Dunlap, G.W. Crabtree, Phys. Rev. B 31 (1985) 49.
[5] S.S. Saxena, P. Agarwal, K. Ahilan, F.M. Grosche, R.K.W. Haselwimmer, M.J. Steiner, E. Pugh, I.R. Walker, S.R. Julian, P. Monthoux, G.G. Lonzarich, A. Huxley, I. Sheikin, D. Braithwaite, J. Flouquet, Nature 406 (2000) 487.
[6] N.D. Mathur, F.M. Grosche, S.R. Julian, I.R. Walker, D.M. Freye, R.K.W. Haselwimmer, G.G. Lonzarich, Nature 394 (1998) 39–43.
[7] M. Yazdani-Kachoei, S. Jalali-AsadabadiIftikhar Ahmad, Kourosh Zarringhalam, Sci. Rep. 6 (2016) 31734.
[8] S. Jalali-Asadabadi, Phys. Rev. B 75 (2007) 205130.
[9] S. Jalali-Asadabadi, F. Kheradmand, J. Appl. Phys. 108 (2010) 073531.
[10] S. Jalali-Asadabadi, S. Cottenier, H. Akbarzadeh, R. Saki, M. Rots, Phys. Rev. B 66 (2002) 195103.
[11] S. Zwirner, V. Ichas, D. Braithwaite, J.C. Waerenborgh, S. Heathman, W. Potzel, G.M. Kalvius, J.C. Spirlet, J. Rebizant, Phys. Rev. B 54 (1996) 12283.
[12] V. Sechovsky, L. Havela, E.P. Wohlfarth, K.H.J. Buschow-North-Holland, Amsterdam, vol. 4, 1988, p. 310.
[13] S. Lebègue, P.M. Oppeneer, O. Eriksson, Phys. Rev. B 73 (2006) 45.
[14] D. Aoki, P. Wiśniewski, K. Miyake, N. Watanabe, Y. Inada, R. Settai, E. Yamamoto, Y. Haga, Y. Ōnuki, J. Phys. Soc. Jpn. 68 (1999) 2182.
[15] M. Zarshenas, S. Jalali-Asadabadi, Thin Solid Films 520 (2012) 2901.
[16] S. Zwirner, V. Ichas, D. Braithwaite, J.C. Waerenborgh, S. Heathman, W. Potzel, G.M. Kalvius, J.C. Spirlet, J. Rebizant, Phys. Rev. B 54 (1996) 12283.
[17] J.P. Sanchez, M.N. Bouillet, E. Colineau, A. Blaise, M. Amanowicz, P. Burlet, J.M. Fournier, T. Charvolin, J. Larroque, Physica B 186 (1993) 675.
[18] A.L. Cornelius, A.J. Arko, J.L. Sarrao, J.D. Thompson, M.F. Hundley, C.H. Booth, N. Harrison, P.M. Oppeneer, Phys. Rev. B 59 (1999) 14473.
[19] P. Boulet, E. Colineau, P. Javorský, F. Wastin, J. Rebizant, J. Alloy. Compd. 394 (2005) 93.
[20] A. Andreev, V.K. Belov, A. Deriagin, V.Z.A. Kazeĭ, R.Z. Levitin, A. Meňovský, Yu. F. Popov, V.I. Silant'ev, JETP 48 (1978) 1187.
[21] A.C. Lawson, A. Williams, J.L. Smith, P.A. Seeger, J.A. Goldstone, J.A. Rourke, Z. Fisk, J. Magn. Magn. Mater. 50 (1985) 83.
[22] E. Ghasemikhah, S. Jalali-Asadabadi, I. Ahmad, M. Yazdani-Kachoei, RSC Adv. 5 (2015) 37592.
[23] F.H.M. Cavalcante, L.F.D. Pereira, J.T. Cavalcante, H. Saitovitch, A.W. Carbonari, R.N. Saxena, M. Forker, J. Appl. Phys. 17 (2013) 113.
[24] M. Forker, P.R.J. Silva, J.T. Cavalcante, F.H.M. Cavalcante, S.M. Ramos, H. Saitovitch, E.B. Saitovitch, R. Alonso, M. Taylor, L.A. Errico, Phys. Rev. B 87 (2013) 159911.
[25] J. Autschbach, D. Peng, M. Reiher, J. Chem. Theory Comput. 8 (2012) 4239.
[26] F. Aquino, N. Govind, J. Autschbach, J. Chem. Theory Comput. 6 (2010) 2669.
[27] S.M. Baizaee, A. Pourghazi, Phys. B. Condens. Matter 358 (2005) 247.
[28] P. Blaha, K. Schwarz, Phys. Rev. B 37 (1988) 2792.
[29] E.N. Kaufmann, R.J. Vianden, Rev. Mod. Phys. 51 (1979) 161.
[30] R. Vianden, Hyperfjtne Interact. 15 (1983) 189.
[31] T. Wichert, E. Recknagel, in: U. Gonser (ed.), Springer-Verlag, BerlinSpringer, vol. 40, 1986, p. 317.
[32] T. Klas, J. Voigt, W. Keppner, R. Wesche, G. Schatz, Phys. Rev. Lett. 57 (1986) 1068.
[33] K. Schwarz, P. Blaha, G. Madsen, Comput. Phys. Commun. (2002) 71.
[34] P. Blaha, K. Schwarz, G. Madsen, D. Kvasnicka, J. Luitz, WIEN2k Code, Vienna University of Technology, Inst. of Physical and Theoretical Chemistry, Getreidemarkt 9/156, A-1060 Vienna/Austria.
[35] J.P. Perdew, A. Zuanger, Phys. Rev. B 23 (1981) 5048.
[36] J.P. Perdew, K. Burke, M. Ernzerhop, Phys. Rev. Lett. 77 (1996) 3865.
[37] V.I. Anisimov, J. Zaanen, O.K. Andersen, Phys. Rev. B 44 (1991) 943.
[38] V.I. Anisimov, F. Aryasetiawan, A.I. Lichtenstein, J. Phys: Condens. Matter 9 (1997) 767.
[39] V.I. Anisimov, O. Gunnarsson, Phys. Rev. B 43 (1991) 7570.
[40] A.B. Shick, Phys. Rev. B 15 (1999) 10763.
[41] A.D. Becke, J. Chem. Phys. 98 (1993) 5648.
[42] A.D. Becke, Phys. Rev. A 38 (1988) 3098.
[43] C. Lee, W. Yang, R.G. Parr, Phys. Rev. B 37 (1988) 785.
[44] S.H. Vosko, L. Wilk, M. Nusair, Can. J. Phys. 58 (1980) 1200.
[45] A.D. Becke, J. Chem. Phys. 98 (1993) 5648.
[46] S. Ayaz Khan, P. Blaha, H. Ebert, J. Minár, O. Šipr, Phys. Rev. B 94 (2016) 144436.
[47] D.D. Koelling, B.N. Harmon, J. Phys. C 10 (1977) 3107.
[48] A.H. MacDonald, W.E. Picket, D.D. Koelling, J. Phys. C 13 (1980) 2675.
[49] J. Kuneš, P. Novák, R. Schmid, P. Blaha, K. Schwarz, Phys. Rev. B 64 (2001) 153102.
[50] N.V.C. Shekar, P.C. Sahu, V. Kathirveland, S. Chandra, Indian J. Phys. 11 (2012) 971.
[51] F. Birch, Phys. Rev. 71 (1947) 809.
[52] P. Novák, J. Kuneš, L. Chaput, W.E. Pickett, Phys. Status Solidi B 243 (2006) 563.
[53] A.V. Kolomiets, L. Havela, V. Sechovský, P. Javorský, J. Kamarád, N. Sato, T.D. Cuong, Phys. B: Condens. Matter 259 (1999) 238.
[54] P. Novák, Calculation of Hyperfine Field in WIEN2k. Technical (2006), 2006.
[55] S. Blügel, H. Akai, R. Zeller, P.H. Dederichs, Phys. Rev. B 35 (1987) 3271.
[56] K. Katrin, K. Koepernik, D.V. Neck, H. Rosner, S. Cottenier, Phys. Rev. A 81 (2010) 032507.
[57] D. Torumba, P. Novák, S. Cottenier, Phys. Rev. B 77 (2008) 155101.
[58] P. Ravindran, A. Delin, P. James, B. Johansson, J.M. Wills, R. Ahuja, O. Eriksson, Phys. Rev. B 59 (1999) 15680.
[59] J. Yu, A.J. Freeman, R. Podloucky, P. Herzig, P. Weinberger, Phys. Rev. B 43 (1991) 532.
[60] S. Zhu, X. Li, Z. Lu, G. Wang, W. Shu, China Institute of Atomic Energy, P.O. Box 275-50, Beijing 102413, PR, 2008.
[61] E.S. Zijlstra, J. Kortus, M. Krajci, Z.M. Stadnik, S.K. Bose, Phys. Rev. B 69 (2004) 94206.
[62] D.R. Torgesonand, F. Borsa, Phys. Rev. B 37 (1976) 956.
[63] M. Jamal, S.J. Hashemifar, H. Akbarzadeh, J. Magn. Magn. Mater. 322 (2010) 3841–3850.
[64] N.J. Stone, Clarendon Laboratory, Oxford, OX1 3 PU, UK, 1999.